Research Article

Experimental Investigation on the Performance of a Dehumidifier Constructed from a Water-to-Air Heat Exchanger Coated with Composite Desiccant of Mesoporous Silica Gel and LiCl

Jintana Srimuk, Surapong Chirarattananon* and Pipat Chaiwiwatworakul
The Joint Graduate School of Energy and Environment, King Mongkut's University of Technology Thonburi, Bangkok, Thailand

Adisak Nathakaranakule, Pattana Rakkwamsuk and Siriluk Chiarakorn
School of Energy, Environment, and Materials, King Mongkut's University of Technology Thonburi, Bangkok, Thailand

* Corresponding author. E-mail: surapong.chi@kmutt.ac.th DOI: 10.14416/j.asep.2023.05.003
Received: 27 January 2023; Revised: 22 February 2023; Accepted: 10 April 2023; Published online: 8 May 2023

Abstract
Thermal environment in buildings in hot climate is conditioned for comfort by air-conditioning that is energy intensive. Presently, most air-conditioning systems in Thailand and other countries in Southeast Asia use electricity-driven vapor compression systems to cool down the air to the set-point temperature. However, latent load due to condensation of air humidity forms a large part of the air-conditioning load. This paper presents the results of experiments on a dehumidifier constructed from a water-to-air heat exchanger coated with a composite desiccant of large-pore mesoporous silica gel and LiCl, regenerated by low-temperature hot water. Moisture removal capacity (MRC), dehumidification capacity (DC), thermal coefficient of performance (COPth), and an equivalent air conditioning load of dehumidification (EALD) are comparative quantitative parameters derived from experimental results and are studied in this research. The composite desiccant requires low-temperature water for regeneration and offers a higher rate of vapor adsorption and desorption that leads to a shorter required desiccant dehumidification cycle time. The results demonstrate that the dehumidifier is able to effectively reduce moisture in ventilation air and substantially reduces the cooling load of air-conditioning.

Keywords: Composite desiccant, Desiccant dehumidification, Dehumidifier, Fin-tube heat exchanger, Mesoporous silica gel

1 Introduction

Buildings now account for 40% of all energy use in wealthy countries and this increases every year [1], [2]. Desires for better thermal comfort in buildings are driving up energy demand, which suggests that the amount of energy consumed inside buildings will increase substantially in the next few years. Specifically, for countries in tropical regions such as Thailand, the energy used for air conditioning accounts for nearly 60% of the total energy used by buildings [3]. The latent component makes up to 70% of the overall cooling load [4], [5]. To achieve suitable indoor air quality, air humidity and temperature must be brought under control. Air humidity is an important issue in indoor air quality. Health problems due to excessive moisture in buildings commonly occur [6].

Building moisture control requires extensive consideration [7], but reducing vapor from humid air is a necessary and an essential step in such control. To control temperature and humidity in buildings, vapor compression refrigeration is commonly used that is energy intensive and exacerbates the challenge towards achieving carbon neutrality. In this process, air

passing through a set of cooling coil transfers heat to the coil and its temperature reduces until it reaches the dew point and its vapor condenses. When air humidity reaches the desired level, its temperature becomes too low and heating is required before the air is supplied into the space [8]. Desiccant dehumidification, on the other hand, operates on the fundamental mechanism of adsorption of moisture from ambient air. Zheng *et al.* [8], extols the merit of energy saving potential of thermo-responsive desiccants. Generally, solid desiccants such as zeolite, silica gel, and molecular sieve have been utilized in air dehumidification systems to control air humidity [9]. When air with higher temperature and humidity flows over the cooler and dry desiccant, moisture from the air is adsorbed. This increases the moisture content as well as the temperature of the desiccant. The desiccant must be heated in the next stage to release the adsorbed water vapor in the process of desorption, or regeneration, then cooled down to reduce its vapor pressure to recover its ability to adsorb moisture again, [10]. It should be noted that desiccant releases heat during the sorption process, which gives rise to more irreversibility loss [5].

The feasibility of the use of low-temperature heat for the regeneration of desiccant is an attraction, Rambhad *et al.* [10], Saeed and Al-Alili [11], Ramli *et al.* [12], Abd-Elhady *et al.* [13]. In household and commercial applications, solid desiccant is preferred, as liquid desiccants are capable of reacting with moist air, and has the potential to create harmful effects for the occupants, [12]. Lower required temperature for regeneration and adsorption capacity are properties considered in the choice of desiccants for air dehumidification in addition to the shape of the desiccant isotherm. In comparison with molecular sieve and activated alumina, silica gel stands out as having high regeneration rate and energy efficiency, [13]. More recently, mesoporous silica receives preference over traditional silica because of its high porosity, low cost, and stability, [5], but even the newer desiccant has a limited moisture adsorption capacity of 35%. One method to increase water vapor sorption capacity of desiccant materials is to impregnate hygroscopic salts such as lithium chloride (LiCl) and calcium chloride ($CaCl_2$) into the desiccant pore. Jiang *et al.* [14] experimented with infused LiCl solution of different mass fractions in mesoporous silica while Hu *et al.* [15], experimented with both LiCl and $CaCl_2$ impregnated silica gel. Both found that both composite desiccants had increased sorption capacity over that of simple silica gel of 30–45%. Hu *et al.* concluded that the composite desiccant of silica gel and LiCl has larger water uptakes than that of the composite desiccant of Silica gel and $CaCl_2$, while Jiang *et al.* concluded that a higher mass fraction of LiCl in the composite desiccant afforded higher sorption capacity, but the solubility limit of LiCl was 40%.

Composite desiccants formed from impregnation of dissolved halide salt in the pores of mesoporous silica gel are considered thermo-responsive desiccants. These have higher vapor adsorption capacity and lower regeneration temperatures than those of simple silica gel desiccants [9], [16].

Channoy *et al.* [17], describes development of a dehumidifier formed from a heat sink coated with mesoporous silica gel, type 3A, impregnated with lithium chloride solution. The dehumidifier is attached to a thermoelectric module charged to different voltages. The dehumidifier was able to achieve a dehumidification capacity of 0.117 kg/h at a charging voltage of 9 V. The physical properties and water sorption kinetics of the composite desiccant of Channoy *et al.* and Zheng *et al.* [9], are similar.

Jiang *et al.* [14], use simple and composite desiccants similar to those in [9], to coat on heat exchangers with aluminium fins to form desiccant dehumidifiers. Hot water at 40 to 60 °C was used during regeneration and cooling water at 15 to 25 °C was used during dehumidification. It was found that the dehumidifier with composite desiccant has higher values of performance indices than the one with simple desiccant.

Hu *et al.* [15], investigates dehumidification capacity and cooling capacity of heat exchanger coated with simple and composite desiccants as functions of regeneration temperature, cooling water temperature (during cooling and dehumidification), speed and condition of inlet air, while Jiang *et al.* [14], considers coefficient of performance (COP) and moisture removal capacity of the same types of dehumidifiers against the same independent variables, as well as the duration of dehumidification period.

In practical applications, the regeneration water (hot) and the cool water used during dehumidification need to be sourced by some means. Wang *et al.* [18],

experimented successfully with the use of solar vacuum tube collectors to produce hot water to regenerate a desiccant coated heat exchanger. The cooling water needed during the dehumidification period was produced by a humidifying cooler that utilizes the dehumidified air from the setup. Zhao *et al.* [19], illustrates through the use of a mathematical model of the mechanisms of operation of a desiccant cooling system utilizing an evaporative cooler (cooling tower) to regenerate cooling water for the cooling system. Chai *et al.* [20], experimented with an air dehumidifier based on the use of desiccant coated heat exchanger and heat pump and found that the setup was able to perform well in ventilation and dehumidification with high energy efficiency.

This paper presents results of experiments to evaluate performance of a dehumidifier fabricated from a heat exchanger coated with composite desiccant, similar to those used in references [9], [14], [15], [18], [19], except that the mesoporous silica gel used in the dehumidifier of this paper has larger pore of 15 nm that results in shorter dehumidifying and regeneration time periods. The average humidity removed by the fabricated dehumidifier in the recommended dehumidification period is significant. The resultant dehumidifier has the potential to be developed for practical employment that utilizes low-temperature and low-cost heat sources.

2 Preparation of the Composite Desiccant of Large Pore Silica Gel with LiCl and its Water Sorption Isotherms

This section describes the steps in the preparation of the composite desiccant and presents graphs of water sorption isotherms of the desiccants.

2.1 *Preparation of the solid composite desiccant*

The silica gel used as the host for the composite desiccant in the experiments in this paper has a pore size of 150 Å (15 nm) and is supplied by Sigma-Aldrich. The silica gel was immersed in an aqueous solution of Lithium Chloride (LiCl) with a mass concentration of 40% by weight of LiCl. The immersion was left for 24 h. The impregnated desiccant was then cleaned in deionized water and left to dry in an autoclave set to 100 °C until its weight did not change. The LiCl content in the desiccant was determined by weight as 38.6%, dry-basis, of the silica gel. The composite desiccant, labeled L40, would be deposited on the heat exchanger in the following step. Note that the simple desiccant (mesoporous silica gel without impregnation of LiCl) is labeled L0 in this paper. Specific surface area (m^2/g) and pore volume (cm^2/g) for L0 and L40 were obtained by specific surface analyzer (supplied by BEL JAPAN, ING., model Belsorp mimi II) as 293 (area) and 1.10 (volume) and 156 and 0.62 respectively. The pore diameter for both L0 and L40 do not differ from 15 nm to any significant extent. Jia *et al.* [21], demonstrated that at high relative humidity, the adsorption capacity of the composite desiccant material is approximately more than three times that of silica gel. There are three different kinds of sorption mechanisms: 1) traditional heterogeneous adsorption on the pore surface, 2) chemical reaction resulting in the formation of salt crystalline hydrates, and 3) liquid adsorption.

In contrast to the method used in this paper, Jiang *et al.* [14], bonded their silica gel (with empty pores) on to the heat exchanger first before impregnating the pores with LiCl solution.

2.2 *Water adsorption isotherms of the composite desiccant*

The method to obtain water sorption isotherms of the desiccant in this paper is to put samples of dry desiccant in a chamber of controlled temperature and relative humidity under atmospheric pressure until the moisture content in the desiccant reaches equilibrium with the air in the chamber. In each experiment, 3 g of simple and composite desiccant was packed in a bag of nylon mesh (mesh size 500) and left to dehydrate in an oven with a temperature set to 100 °C for 24 h before adsorption isotherm testing. The samples were then put in a constant temperature and humidity chamber (supplied by DAEYANG ETS, model TH180-S, stability: temperature ±0.1 °C, RH ±3%). Three temperature values were set: 30, 50, and 70 °C at each of which five relative humidity values, 10, 30, 50, 70, and 90% were set. The samples were left in the chamber for each condition until the weights did not change that in each condition took a few hours. Finally, the equilibrium water content was determined by weighing the samples to obtain the equilibrium isotherms.

The markers in the graphs in Figure 1 show the

results from the tests described in the last paragraph. The set with filled square markers corresponds to those for L40 at 70 °C and forms the isotherm for the composite desiccant at 70 °C. Those with empty square markers form the isotherm for the simple desiccant at 70 °C. The points represented by the triangular and the round markers correspond to the isotherms for composite and simple desiccants at 50 and 30 °C respectively. Using multinomial curve fitting of polynomial order 3 for the relative humidity and order 2 for the temperature, the results are shown in solid line for the isotherm of composite desiccant and dotted lines for the simple desiccant at the three temperature values. The multinomial curve fitting form used is also known as the 'double log polynomial model, DLP. The coefficients of determination for each case in Figure 1 is higher than 0.995.

Note that the moisture content of the simple desiccant reaches about 38% at the air relative humidity of 90% and the temperature of 30 °C, while for the composite desiccant, it reaches 71%. These are consistent with those observed in [9], [22].

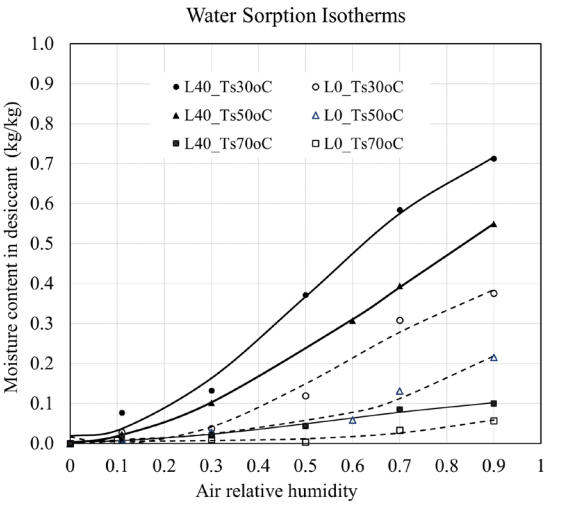

Figure 1: Isotherms at different temperatures for the composite and the simple desiccant.

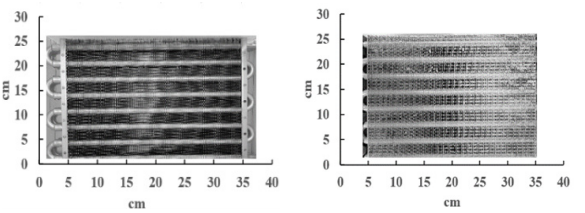

Figure 2: Photographs of the fin-tube heat exchanger without (a) and with (b) composite desiccant.

3 Deposition of the Desiccant and Forming and Testing the Composite Desiccant Dehumidifier

Examining graphs of the water absorption isotherms in Figure 1, it was deemed that composite desiccant would likely form a better functioning dehumidifier, and thus the composite desiccant would be used and tested in the dehumidifier setup. The first step would be to coat and bond the composite desiccant on the heat exchanger, then fabricate the dehumidifier. For the experiment, there are testing conditions to consider.

3.1 *Deposition of the composite desiccant on the fin-tube heat exchanger*

An off-the-shelf commercial fin-tube heat exchanger (HX) was selected for use in the experiments. Figure 2(a) shows a photograph of the HX. Its dimensions are: length 300 mm, width 260 mm, and depth 20 mm. The thickness of the aluminum fin is 0.5 mm and the diameter of the aluminum tube is 6.31 mm. The HX has a single water tube and no header. The HX was cleaned with a distilled water wash and placed in an oven at 100 °C for 1 h. The cleaned and dried HX was then dipped in a polyurethane binder, after which the composite desiccant was deposited, and the binder was polymerized with ultraviolet radiation for 24 h. A photograph of the fin-tube heat exchanger with deposited composite desiccant is shown in Figure 2(b).

A section of the desiccant deposited HX was photographed under a scanning electron microscope (SEM). Figure 3 shows photographs of the section with two different magnification levels. The desiccant particles appeared close and sufficiently densely packed.

As described in Subsection 3.2, two frames of HX stack were packed together to perform as one stack. The mass of the desiccant and binder on a stack of two frames of HX weighed 132.68 and 31.83 g, respectively.

As noted in Section 2, the method of preparation of the composite desiccant and depositing it on the HX described above differs from that described in [14].

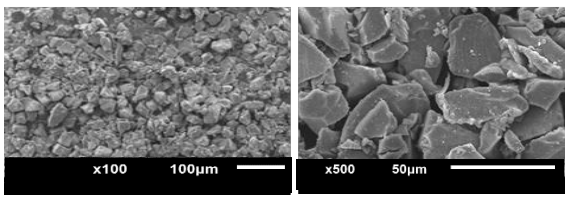

(a) 100x (b) 500x

Figure 3: SEM photographs of composite desiccant coated fin at two different magnifications.

3.2 *Fabrication of the desiccant dehumidifier*

The HX with deposited composite desiccant would perform the function of a dehumidifier when air passes through it during the dehumidification period, and air is needed to pass through it to remove moisture from the desiccant during the regeneration period. The condition of air that moves into and out from the HX needs to be measured under the condition of non-turbulent air flow, for which air ducts are needed to promote orderly air flow. In the experiments reported in this paper, ambient air enters at an entry port in one location, to pass through a duct, through the HX, and through another duct for exhausting air out through the ambient exit port at another location.

Figure 4 shows the schematic diagram of a complete dehumidifier. The dehumidifier comprises two sets of composite desiccant HX, or CDHX. In operation, a CDHX operates to dehumidify air when cool water flows in the tube in one period, while another CDHX regenerates the desiccant with hot water at the same time period. A CDHX operates as a dehumidifier in a dehumidification period, then operates to regenerate its desiccant in an alternate period. The time duration of the two periods is equal and together form a cycle. The hot water is supplied from a tank to both CDHX on alternate periods, and similarly for cool water. Electrically operated three-way valves were used to direct both hot water and cool water alternately in and out of the tube of a CDHX.

Each CDHX used comprises two HX stacked in series, with the water tubes also connected in series for a total stack depth of 40 mm. The dehumidifier fabricated and experimented on in this paper uses low power axial fans and pumps.

Two multi-function digital thermo/hygrometers (KIMO, 210-R, accuracy 0.25 °C and 1.5% RH) were used to measure temperature and humidity ratio of air at the inlet and outlet to a DCHX. Air speed was measured by an anemometer (KIMO, CTV 110). A PT-100 sensor with an accuracy of 0.1 °C was inserted between two fins of the CDHX stack to measure the temperature of the fins and desiccant. Water temperatures were measured by PT-100 sensors, and A floating meter was used to measure the flow rate of water. The positions of all sensors are shown in Figure 4. A data logger (NIcDAQ-9188) was used to record all measurements with an interval of 5 s. The flow of water was controlled to 0.10526 L/s or 6.32 L/h. This rate of flow for water was kept the same for all experiments, while that of air was primarily set to 0.83 m/s, but was varied in a set of experiments.

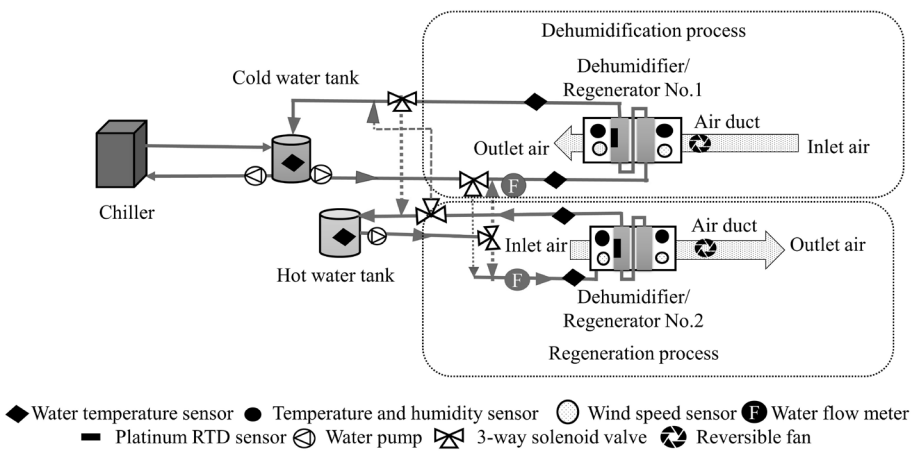

Figure 4: Schematic diagram of the experimental setup.

3.3 *Conditions of air during experiments*

The experiments were carried out in a laboratory in Bangkhuntian Campus of KMUTT, located in a sparse suburban area close to the sea. Ambient air was used in all experiments. There was no rain, the sky was clear, and the weather was calm throughout the duration of each set of experiments. Although the experiments were conducted on different days in October and December of 2022, the condition of the air during the experiments fell roughly into two conditions. In Condition 1, the temperature was 33 °C and its humidity ratio was 19 g/kg of dry air (relative humidity was 60%) and in Condition 2, the temperature was 31 °C and its humidity ratio 14 g/kg of dry air (relative humidity 50 %).

The temperature of the cool water was fixed at 30 °C. The temperature range of the hot water was from 40 to 70 °C, in each step of 10 °C. The duration of period of dehumidification varies from 1 min or 60 s to 4 min or 240 s. One set of experiments was conducted with air in Condition 1. Most experiments were conducted with air in Condition 2.

4 Results and Discussion

All the experiments reported here were conducted with only one set of CDHX that operated alternatively in a regeneration period followed by a dehumidification period. The graphs in Figure 5 show values of temperatures and humidity ratios of air for 3 consecutive periods of regeneration, dehumidification, and regeneration. The time duration of each period in Figure 5 is 2 min or 120 s. The air in this set of experiments belongs to Condition 1. Temperature values appear on the upper part of the vertical axis, while those of humidity ratios appear on the lower part. The horizontal axis shows the time in seconds. The graphs show values of temperatures of water in the tube (in square markers) at the point of entering (filled markers, Twin), and at the point of leaving the CDHX (hollow markers, T_{wout}), of ambient air that flows into the CDHX (filled triangular markers, $T_{gin,amb}$), of air that flows out from the CDHX (empty triangular markers, T_{gout}) and of the desiccant coated fins (grey diamond marker, T_s). The values of the humidity ratio of ambient air at entry, $W_{gin,amb}$, are represented by filled round markers and those of the humidity ratio of ambient air at the exit, W_{gout}, are represented by empty round markers.

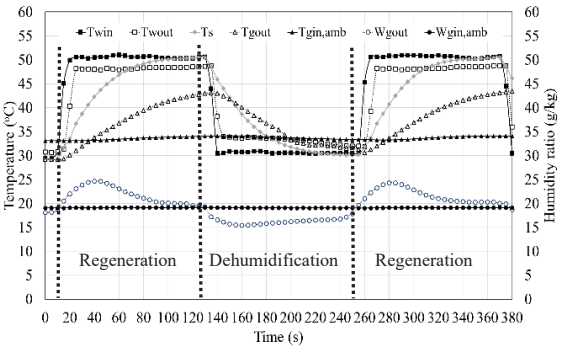

Figure 5: Graphs of temperatures of air and water and humidity ratios of air when the temperature of regeneration water is 50 °C and the duration of each period is 2 min.

4.1 *Dynamics of regeneration (and dehumidification)*

During regeneration, the three-way valve directs hot water into the CDHX to replace the cool water in the water tube from the previous dehumidification period. A certain time duration is required before hot water reaches the end of the tube and completely replaces the cool water. In Figure 5, a small time lag is observed between the instant the temperature of hot water at the entry of the tube reaches its final value of 50 °C and the instant the temperature at the outlet of the tube reaches its final value of 48 °C. When hot water begins to flow into the tube in the HX housing, it commences transferring heat to it. The thermal mass of the housing and of the desiccant contribute to dynamic change (delayed rise) of temperature, T_s, measured by the sensor at the desiccant coated fins. It is seen that this temperature seems to reach its final value, close to 50 °C, by the end of the period. Heat is transferred from the fins and tube of the HX housing to the air mainly by convection. The air temperature at the end of each period reaches about 43 °C, but it seems as if it keeps rising further if the duration of the period is extended, signifying that the time constant of this dynamic is longer than the duration of 2 min.

The humidity ratio of air seems as if to increase, signifying the release of moisture from the composite desiccant into the air, at the instant hot water enters into the CDHX. The air humidity ratio keeps rising to reach its peak at 30 s after the beginning of the period

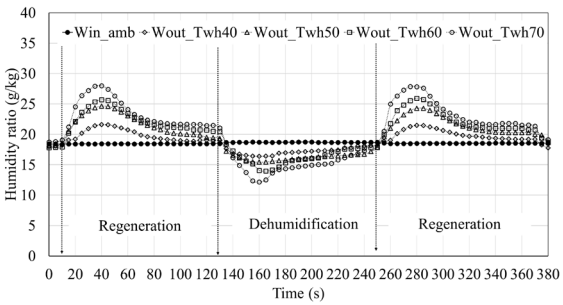

Figure 6: Levels of humidity ratios at the inlet and outlet air under the different regeneration water temperatures but with the identical condition of inlet air and operating condition of that in Figure 5.

and then declines. This decline signifies that moisture in the desiccant has reduced to the point that the rate of vaporization has slowed. However, by the end of the period, there is still some observable vaporization. During the period of adsorption or dehumidification of air, the pattern of air humidity reduction does not seem to be quite symmetrical to the pattern of its increase in the regeneration period. There is more uniformity in the level of adsorption and by the end of the period, the level of adsorption seems rather significant still.

The rate of vapor released from desiccant into the air that is measured as air humidity ratio in the regeneration period in Figure 5 corresponds to the hot regeneration water temperature of 50 °C. Figure 6 shows the different levels of air humidity ratio that correspond to regeneration water at other temperatures.

In Figure 6, the graph with filled round markers represents the pattern of humidity ratio of inlet air, W_{in_amb}, that with empty diamond markers of humidity ratio of air with regeneration water temperature of 40 °C, W_{out} *_Twh40*, that with empty triangular markers of humidity ratio of air with regeneration water temperature of 50 °C, W_{out}*_Twh50*, that with empty square markers of humidity ratio of air with regeneration water temperature of 60 °C, W_{out} *_Twh60*, and that with empty round markers of humidity ratio of air with regeneration water temperature of 70 °C, W_{out} *_Twh70*. The levels of humidity ratios of air rise progressively with higher regeneration temperatures. Overall, the patterns of humidity ratios during regeneration and dehumidification in Figure 6 appear to be more symmetrical.

At the end of the regeneration period, the humidity ratio of the outlet air still seems to be higher than that of the inlet air implying that there is remaining moisture from the desiccant and it is still being vaporized. Conversely, at the end of the dehumidification period, there seems to be continuing adsorption of vapor of the air by the desiccant. These observed phenomena imply that given a longer time duration, the desiccant would become dryer (less adsorbed moisture) from regeneration and would adsorb more vapor during dehumidification. Given longer time periods for regeneration and dehumidification, the desiccant would reach closer to its eqilibrium condition, and vice and versa, given shorter time periods, the desiccant would be further from its eqilibrium condition.

4.2 *Indices of dehumidification performance*

The effectiveness and performance of a CDHX operating as a dehumidifier are the main interest of this paper. The last subsection notes the effect of the temperature of the regeneration water on the level of vaporization and removal of moisture from the composite desiccant and conversely, the effective adsorption of vapor from air by the desiccant.

Vivekh *et al.* [5], and Jiang *et al.* [14], define the transient difference between the humidity ratio of air at the outlet, W_{gout} and that at the inlet, W_{gin} of a CDHX operating as a dehumidifier as the moisture removal,

$$D_t = W_{gout} - W_{gin},$$

The time average of the moisture removal is defined as the moisture removal capacity, MRC, as expressed in the following Equation (1).

$$MRC = \frac{1}{d_t}\int_0^{d_t} D_t dt \quad (1)$$

where d_t is the time period of dehumidification. Both quantities D_t and *MRC* have the same unit as that of humidity ratio, g/kg or kg/kg. Both reference papers define dehumidification capacity, *DC*, as the rate that the air carries vapor away, as shown by the ensuing Equation (2),

$$DC = \dot{m}_a(MRC) \quad (2)$$

where $\dot{m}_a$ is the mass flow rate of air, kg/s, and *DC* has the unit of g/s or kg/s.

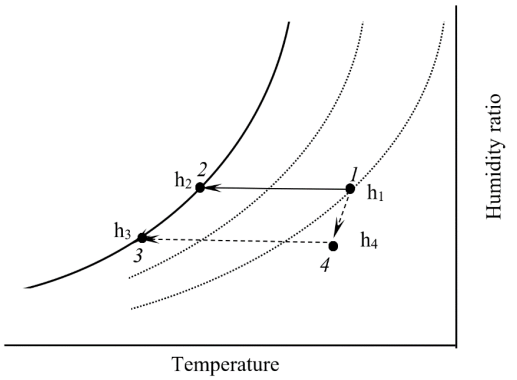

Figure 7: Illustration of the process of air dehumidification by a CDHX and by an air-conditioner [17].

In air-conditioning via vapor compression, the air is cooled by a cooling coil commonly beyond the dew point temperature so that some vapor of the air that passes through the cooling coil condenses and its air humidity ratio is reduced. Figure 7 illustrates the processes of desiccant dehumidification and air-conditioning on a psychrometric chart. Point 1 corresponds to condition of air at inlet. Point 4 is the condition of air that has passed through a CDHX dehumidifier and its humidity ratio has been reduced by $\Delta W = W_1 - W_4$. The process that air passing through the cooling coil is cooled down to reach the dew-point temperature is represented by the path from point 1 to point 2. Further passage of air through the coil causes condensation of its vapor, and its humidity ratio reaches that at point 3, where the humidity ratio is identical to that of point 4, $W_3 = W_4$. If the enthalpy of air at point 3 is h_3 and that at point 1 is h_1, then the cooling load to the air-conditioner to bring air from point 1 to point 3 is $\dot{m}_a(h_1 - h_3)$. This is the equivalent air-conditioning load, EALD, achieved by the dehumidifier in reducing the humidity of air at point 1 to point 3, as demonstrated by the Equation (3) that follows,

$$EALD = \dot{m}_a(h_1 - h_3) \tag{3}$$

If the enthalpy of air at point 4 is h_4, then the output thermal load achieved by the dehumidifier in bringing air at the condition at point 1 to the condition at point 4 is the dehumidification capacity of the CDHX performing as a dehumidifier Q_d, where

$$Q_d = \dot{m}_a(h_1 - h_4)$$

This output results from using hot water at temperature T_{win} to feed into the coil of the CDHX where the temperature of the leaving hot water becomes T_{wout}. If the specific heat of water at constant pressure is c_{pw}, then the thermal heat exchange rate of hot water at input Q_w, is

$$Q_w = \dot{m}_w c_{pw}(T_{win} - T_{wout})$$

Reference [5] and [14] defines the ratio of an analogous quantity to Qd (when the CDHX operates to cool air) to Q_w as the thermal coefficient of performance of cooling. Here, the ratio of Q_d to Q_w is defined as the thermal coefficient of performance of dehumidification, as indicated in the Equation (4) below,

$$COP_{th} = \frac{Q_d}{Q_w} \tag{4}$$

4.3 *Factors affecting performance of CDHX dehumidifier*

The research undertaken and the experiments conducted as described here were based on a belief that it is feasible that CDHX fabricated as described in Section 3 could be practically used as a dehumidifier that utilizes low-cost and low carbon energy sources, such as that from solar water heaters. The experimental results presented in Subsection 4.1 that hot water at 40 °C could be used to regenerate the composite desiccant reinforces the belief. It is of interest next to examine what factors and how these factors affect the performance of the CDHX fabricated, given the two conditions of input air used, as described in Subsection 3.3, and given that the temperature and flow rate of the cool water used during dehumidification is kept to 30 °C and 6.32 L/h.

4.3.1 Effect of hot water temperature and duration of regeneration (and dehumidification) period

It is observed in Figure 6 that during the regeneration period, the desiccant has desorbed its moisture substantially, yet it is still desorbing, even at a low rate, by the end of the period. If the duration of the period is reduced while the desorption rate is high in the reduced duration, the average rate of desorption could be

higher. Inversely, if the duration is longer, the average desorption rate could be lower. The experiments that produce results in Figure 6 were conducted based on air in Condition 1.

Figure 6 shows clearly that the higher regeneration water temperature produces higher desorption of moisture from the desiccant, but the results are all from the same set of experiments where the duration of regeneration is 2 min. Later experiments were conducted with alternative durations of regeneration period (and dehumidification period). In order to distinguish these experiments of different durations, a label C1 will be used for experiments using a duration of 1 min, C2 for 2 min, etc.

Further experiments were conducted later with the air of Condition 2. In this alternate set of experiments, the duration of each period was set to half of that in the previous set of experiments, of one minute and labeled C1, and the temperature was varied through the full range from 40 to 70 °C.

Upon completion of the experiments of the preceding paragraph, another set was conducted with the air of Condition 2, but with the duration of the period set to 4 min, labeled C4. The temperature of the regeneration water was again varied over the full range of 40 to 70 °C.

The results from all the experiments described above, where air in both conditions are used, with a duration of each period at C1, C2, and C4, and with temperature of hot water varied from 40 to 70 °C, are compiled and the values of MRC, DC, COPth, and EALD plotted in Figures 8–11.

Note that the experiments conducted with a duration of two minutes, designated C2, were under air in Condition 1 where its humidity ratio is 19 g/kg of dry air. All other experiments were under air Condition 2 with a humidity ratio of 14 g/kg.

The three graphs with three different durations but one common regeneration temperature form a cluster in the figure that altogether form 4 clusters. The patterns of all clusters are the same: the value of MRC for C1 is lower than that of C2, but larger than that of C4, and the magnitudes of all clusters increase monotonically with hot water temperature.

The graphs show that, with the same duration, higher regeneration water temperature causes a higher level and faster rate of dehumidification of moisture from the desiccant. Between the three durations with the same temperature, C2 has the highest dehumidification effect as seen from the figure, even though the experiments with C2 were conducted under a certain difference in air condition.

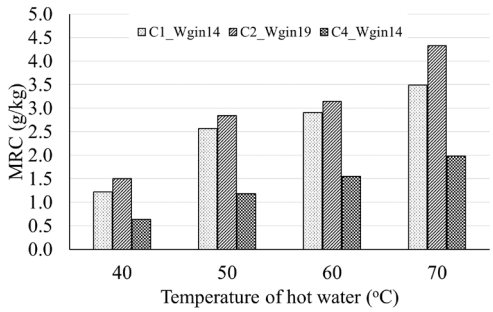

Figure 8: Values of MRC for CDHX dehumidification with duration C1 to C4 at all four temperature levels and under the two air conditions.

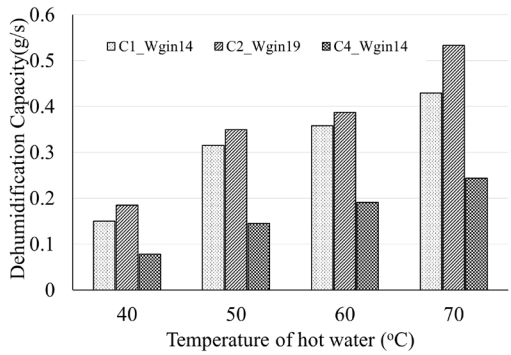

Figure 9: Values of DC for CDHX dehumidification with duration C1 to C4 at all four temperature levels and under the two air conditions.

The patterns in both Figures 8 and 9 are identical. From Equations (1) and (2), each value of DC is obtained from the corresponding value of MRC by multiplying it by a factor of air mass flow rate that is identical for all cases here.

The patterns in Figure 10 are similar but not identical to those of MRC and DC in the preceding two figures. In all cases, the rate of hot and cool water flows into CDHX are identical. In all dehumidification cases, the same cool water temperature was used, thus the values of Qw in (4b) in all cases of the same temperature are similar. While the main components of MRC and DC in all cases are the vapor adsorbed by desiccant or moisture released from the desiccant, the numerator of each COPth term comprises both latent

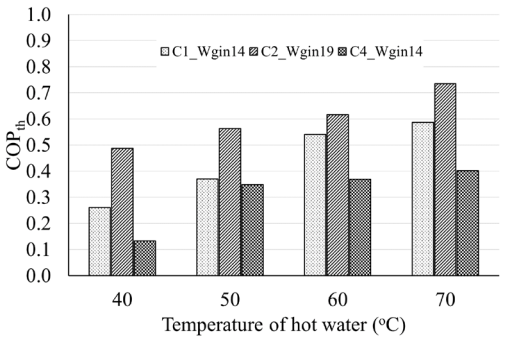

Figure 10: Values of COPth for CDHX dehumidification with duration C1 to C4 at all four temperature levels and under the two air conditions.

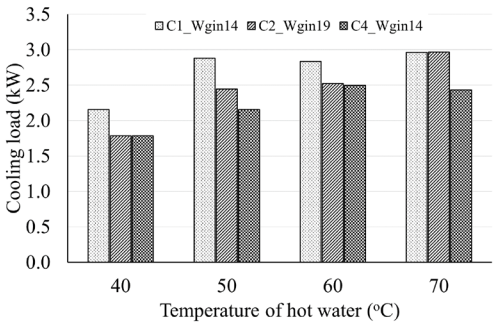

Figure 11: Values of EALD for CDHX dehumidification with duration C1 to C4 at all four temperature levels and under the two air conditions.

and sensible components of the difference between the enthalpy of inlet and outlet air. The heat of adsorption contributes sensible enthalpy to the outlet air and reduces the overall difference. Thus the difference between the COPth of the different clusters with respect to temperature in Figure 10 is not as pronounced as the difference in DC values in Figure 9.

Figure 11 shows values of EALD for the same conditions as in the preceding cases. The patterns in Figure 11 exhibit the effect of hot water temperature, though not as strong as those preceding cases. Within the cases of the same temperature, those with C1 or a duration of one minute seem more pronounced. Examining the composition of EALD in Figure 7, only the enthalpy related to a change in air humidity and thus the latent component contributes clearly to the EALD value. The EALD value is strongly related to the enthalpy of the inlet air.

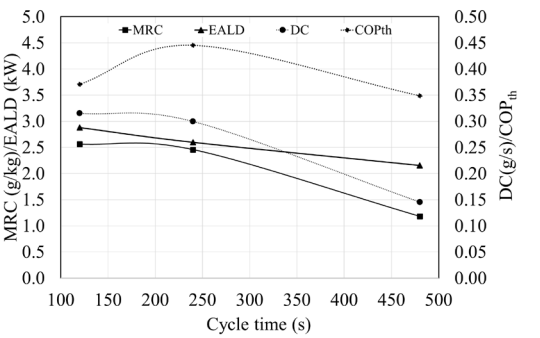

Figure 12: Graphs of MRC, DC, COPth, and EALD VS cycle time in one frame.

Overall, temperature and cycle time have strong influence on the performance indices of MRC and DC, less strong on COPth, and even less on EALD. The C2 duration of regeneration renders higher performance among the 3 durations used in the experiments.

4.3.2 Optimal duration of regeneration (and dehumidification)

The preceding section concludes that the CDHX operating with duration C2 appears to result in better performance of MRC, DC, and COPth indices among the three duration options. However, the experiments from which the indices are constructed were conducted under two different conditions of inlet air. It is of interest to find a more precise duration at which the indices reach the optimum point(s) under the same condition of inlet air, if an optimum duration exists.

Another set of experiments was conducted under the condition of air classified as Condition 2, with a hot water temperature of 50 °C, with cool water temperature and flow rates identical to previous cases but with three durations of generation period. The results were used to derive the four performance indices, their graphs are shown against cycle time (twice of duration) in Figure 12.

Each graph of MRC, DC, and COPth appears to have an optimum point, but at the point of optimum value of each index, the time duration differs from one index to those of others, i.e. no common value of the time duration. However, the mean duration among the graphs, the optimal cycle time, is 207 s. The graph for EALD does not have an optimum point.

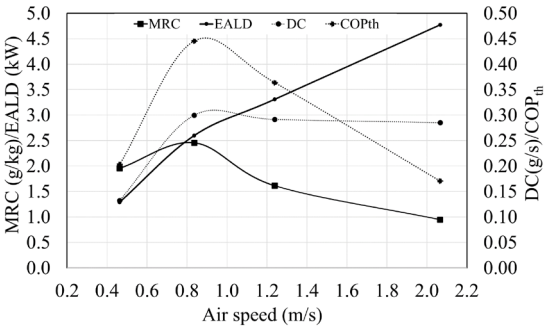

4.3.3 Effects of the speed of air flow

Jiang *et al.* [14], experimented with varying the speed of air flow in a CDHX similar to the one in this paper and found that both MRC and COPth declines gradually with increasing inlet air speed. Hu *et al.* [15], uses their validated mathematical model of their fabricated CDHX to simulate the operation of the model for air cooling and dehumidification. Their graphs show that increasing inlet air speed from a very low value increases DC, but when the speed exceeds about 1.0 m/s, the value of DC declines gradually.

In the same set of experiments described in subsection b but with a fixed duration of 2 min (C2) inlet air speed was varied in a range from 0.46 to 2.01 m/s, the values of the performance indices are calculated from the measurements and graphed as shown in Figure 13.

Similar to the graph presented by Hu *et al.* [15], MRC and DC show that each has an optimum point, although the two points are at a slightly different speed. The graph of COPth also shows that there is an optimum point. All three optimum points are not sharp and the values are between 0.83 to 1.3 m/s. There is no optimum point for EALD.

5 Conclusions

This paper presents the use of mesoporous silica gel to coat on a commercial water-to-air to function as a dehumidifier. Hot water is an effective medium for heat transfer to desiccant that enhances the subsequent desorption of moisture by the desiccant. Laboratory experiments show that the composite desiccant used renders the dehumidifier viable to be used to dehumidify air. It functions with supply hot water at a temperature from 40 °C where it was able to reduce the relative humidity of air at 33 °C, RH 60% to 55%, and for water at 70 °C to 35%. The composite desiccant also requires less cycle time that leads to an increasing reduction of air humidity and reduction of regeneration heat. It is expected that it would be feasible to use the dehumidifier with low cost heat sources and is cost-effective.

Acknowledgments

This research was supported by The Joint Graduate School of Energy and Environment (JGSEE) and International Research Network Program (IRN). In addition, We are most grateful to the faculty of the School of Energy Environment and Material of KMUTT, to Assoc.Prof.Dr.Jatuphorn Wootthikanokkhan, who recommended the binder used, and to the Department of Chemical Engineering of KMUTT, and to Prof. Dr.Ratana Jiraratananon, who suggested the method to obtain adsorption isotherm of composite desiccant.

Author Contributions

J.S.: contributed to the investigation, methodology, data analysis, and writing of the original draft; S.C.: was responsible for conceptualization, ensuring result consistency, writing, reviewing, and editing, funding acquisition, and project administration. All authors have reviewed and approved the final version of the manuscript for publication.

Conflicts of Interest

The authors state that they have no competing interests.

References

[1] L. Pérez-Lombard, J. Ortiz, and C. Pout, "A review on buildings energy consumption information," *Energy and Buildings*, vol. 40, pp. 394–398, 2008, doi: 10.1016/j.enbuild.2007.03.007.

[2] M. González-Torres, L. Pérez-Lombard, J. F. Coronel, I. R. Maestre, and D. Yan, "A review on buildings energy information: Trends, end-uses, fuels and drivers," *Energy Reports*, vol. 8, pp. 626–637, Nov. 2022, doi: 10.1016/j.egyr.2021.11.280.

[3] S. Chirarattananon, "Climate influence on buildings

and end-use energy requirements," The Joint Graduate School of Energy and Environment (JGSEE), Bangkok, Thailand 2019.

[4] F. Zhang, Y. Yin, and X. Zhang, "Performance analysis of a novel liquid desiccant evaporative cooling fresh air conditioning system with solution recirculation," *Building and Environment*, vol. 117, pp. 218–229, May 2017, doi: 10.1016/j.buildenv.2017.03.015.

[5] P. Vivekh, M. Kumja, D. T. Bui, and K. J. Chua, "Recent developments in solid desiccant coated heat exchangers – A review," *Applied Energy*, vol. 229, pp. 778–803, Nov. 2018, doi: 10.1016/j.apenergy.2018.08.041.

[6] P. Wolkoff, "Indoor air humidity, air quality, and health-An overview," *International Journal of Hygiene and Environmental Health*, vol. 221, pp. 376–390, 2018, doi: 10.1016/j.ijheh.2018.01.015.

[7] U.S. Environmental Protection Agency, "Moisture control guidance for building design, construction and maintenance," 2013. [Online]. Available: http:// www.epa.gov/iaq/moisture

[8] Y. Zeng, J. Woods, and S. Cui, "The energy saving potential of thermos-responsive desiccants for air dehumidification," *Energy Conversion and Management*, vol. 244, Sep. 2021, Art. no. 114520, doi: 10.1016/j.enconman.2021.114520.

[9] X. Zheng, T. S. Ge, Y. Yang, and R. Z. Wang, "Experimental study on silica gel-LiCl composite desiccant for desiccant coated heat exchanger," *International Journal of Refrigeration*, vol. 51, pp. 24–32, Mar. 2015, doi: 10.1016/j.ijrefrig.2014.11.015.

[10] K. S. Ramblad, P. V. Walke, and D. J. Tidke, "Solid desiccant dehumidification and regeneration methods – A review," *Renewable and Sustainable Energy Review*, vol. 59, pp. 73–83, Jun. 2016, doi: 10.1016/j.rser.2015.12.264.

[11] A. Saeed and A. Al-Alili, "A review on desiccant coated heat exchangers," *Science and Technology for the Built Environment*, vol. 23, pp. 136–150, 2017, doi: 10.1080/23744731.2016.1226076.

[12] M. S. A. Ramli, S. Misha, N. F. Haminudin, M. A. M. Rosli, A. A. Yusof, M. F. M. Basar, K. Sopian, A. Ibrahim, and A. Z. Abdullah, "Review of desiccant in the drying and air-conditioning application," *International Journal of Heat and Technology*, vol. 39, pp. 1475–1482, Oct. 2021, doi: 10.18280/ijht.390509.

[13] M. M. Abd-Elhady, M. S. Salem, A. M. Hamed, and I. I. El-Sharkawy, "Solid desiccant –based dehumidification systems: A critical review on configurations, techniques, and current trends," *International Journal of Refrigeration*, vol. 133, pp. 337–352, Jan. 2022, doi: 10.1016/j.ijrefrig.2021.09.028.

[14] Y. Jiang, T. S. Ge, R. Z. Wang, and L. M. Hu, "Experimental investigation and analysis of composite silica-gel coated fin-tube heat exchangers," *International Journal Refrigeration*, vol. 51, pp. 169–179, Mar. 2015, doi: 10.1016/j.ijrefrig.2014.11.012.

[15] L. M. Hu, T. S. Ge, Y. Jiang, and R. Z. Wang, "Performance study on composite desiccant material coated fin-tube heat exchangers," *International Journal of Heat and Mass Transfer*, vol. 90, pp. 109–120, Nov. 2015, doi: 10.1016/j.ijheatmasstransfer.2015.06.033.

[16] Y. D. Tu, R. Z. Wang, and T. S. Ge, "Moisture uptake dynamics on desiccant-coated water-sorbing heat exchanger," *International Journal of Thermal Science*, vol. 126. pp. 13–22, Apr. 2018, doi: 10.1016/j.ijthermalsci.2017.12.015.

[17] C. Channoy, S. Maneewan, S. Chirarattananon, and C. Punlek, "Development and characterization of composite desiccant impregnated with LiCl for thermoelectric dehumidifier (TED)," *Energies*, vol. 15, Feb. 2022, Art. no. 1778, doi: 10.3390/en15051778.

[18] H. H. Wang, T. S. Ge, X. L. Zhang, and Y. Zhao, "Experimental investigation on solar powered self-cooled cooling system based on solid desiccant coated heat exchanger," *Energy*, vol. 96, pp. 176–186, Feb. 2016, doi: 10.1016/j.energy.2015.12.067.

[19] Y. Zhao, Y. J. Dai, T. S. Ge, H. H. Wang, and R. Z. Wang, "A high-performance desiccant dehumidification unit using solid desiccant coated heat exchanger with heat recovery," *Energy and Buildings*, vol. 116, pp. 583–592, Mar. 2016, doi: 10.1016/j.enbuild.2016.01.021.

[20] S. Chai, X. Sun, Y. Zhao, and Y. Dai, "Experimental investigation on a fresh air dehumidification system using heat pump with desiccant coated heat exchanger," *Energy*, vol. 19, pp. 306–314, Mar. 2019, doi: 10.1016/j.energy.2019.01.023.

[21] C. X. Jia, Y. J. Dai, J. Y. Wu, and R. Z. Wang, "Experimental comparison of two honeycombed desiccant wheels fabricated with silica gel and composite desiccant material," *Energy Conversion and Management*, vol. 47, pp. 2523–2534, Sep. 2006, doi: 10.1016/j.enconman.2005.10.034.

[22] M. Sultan, I. El-Sharkawyb, T. Miyazaki, B. B. Saha, and S. Koyama, "An overview of solid desiccant dehumidification and air-conditioning," *Renewable and Sustainable Energy Reviews*, vol. 46, pp. 16–19, Jun. 2015, doi: 10.1016/j.rser.2015.02.038.